Single- and multiphoton detachment from stored F^- ions

N. Kwon, P. S. Armstrong, T. Olsson, R. Trainham, and D. J. Larson
Jesse W. Beams Laboratory of Physics, Department of Physics, University of Virginia, Charlottesville, Virginia 22901
(Received 9 March 1989)

The cross sections for one-, two-, and three-photon detachment from fluorine negative ions have been measured using light at the fundamental and harmonic frequencies of a 1064-nm pulsed neodymium-doped yttrium aluminum garnet laser. The ions were stored in a Penning ion trap, the depletion due to illumination was measured, and the data were fitted to a model for stored ions illuminated by pulsed light. The values obtained for the detachment cross sections are $\sigma^{(1)}=2.8(5)\times10^{-18}$ cm^2, $\sigma^{(2)}=2.0(7)\times10^{-50}$ cm^4 sec, and $\sigma^{(3)}=7.9^{+6.6}_{-3.6}\times10^{-83}$ cm^6 sec^2. These values are compared with theoretical calculations and other experimental results.

I. INTRODUCTION

Multiphoton detachment from negative ions holds promise as fertile common ground for atomic theory and experiments. The lack of resonance structure below the one-photon threshold means that the cross sections are not rich in features, but also simplifies some aspects of both calculations and measurements. The halogen negative ions, with electron affinities ranging from 3.0 to 3.6 eV, are well suited for experiments involving the absorption of a small number of visible or near visible photons. Recently, a number of calculations of absolute cross sections for multiphoton detachment from halogen negative ions have been carried out,[1-5] but, to date, few measurements have been performed. Two measurements of absolute cross sections of multiphoton detachment from I^- using ion beams have been reported previously. An early experiment measured two-photon detachment using a ruby laser,[6] and a recent experiment studied three-photon detachment using a neodymium-doped yttrium aluminum garnet (Nd:YAG) laser.[7] Also, Trainham, Fletcher, and Larson have reported approximate values of the absolute cross sections for one- and two-photon detachment from Cl^- stored in an ion trap.[8] That particular measurement concentrated on the behavior of the detachment cross sections near threshold.

In the present paper, we report absolute values of cross sections for one-, two-, and three-photon detachment from F^- ions stored in a Penning ion trap. In the process of carrying out these measurements, the suitability of the ion-trap apparatus for absolute single- and multiphoton cross-section measurements has been examined. Previously, ion traps have been used in a number of experiments which measured relative photodetachment cross sections,[9] including multiphoton cross sections,[10] but we have found only one absolute photon cross section, a photodissociation cross section,directly measured using an ion trap.[11] Photodissociation cross sections have also been measured in an ion-cyclotron-resonance (ICR) spectrometer by comparison to a known cross section.[12] In a number of different experiments, absolute cross sections or rate constants for electron recombination,[13] electron capture or charge exchange,[14] and electron-atom collisions have been measured using ion traps.[15] Radiative association rates have been measured in a Penning trap[16] and extensive studies of ion-molecule reactions have been carried out in ICR cells.[17] Absolute multiphoton cross sections may at first appear to be particularly difficult to measure with ion traps, since the focusing used to produce the necessary light intensities is incompatible with the simplest geometry which consists of uniform illumination of all the ions. However, the present study demonstrates that ion traps can be used effectively for measurements of absolute multiphoton cross sections.

One advantage of using a stored-ion or stored-atom technique is the possibility of obtaining long interaction times between the ions or atoms and the radiation. The long interaction times and high sensitivity make the use of traps attractive for cross-section measurements on rare species and in the case of low light intensities. Unlike measurements with most other techniques, the ideal trap operates as a perfect integrator. Noise appears in the determination of ion number and is independent of integration time. Thus the detachment signal-to-noise ratio grows linearly with interaction time. The dynamic range of the measurements, which is limited in the present case by a total-ion signal-to-noise ratio of about 50, can be extended by varying the interaction time.

In our experiments, photodetachment is measured by obtaining the ratio of the ion number in the trap after laser illumination to the initial ion number. A measurement of the absolute number of ions is not necessary in order to obtain the absolute cross section for a photodetachment process. As in other types of experiments, the cross section can be obtained from a knowledge of the light power and spatial distribution alone if the detachment signal is measured as a function of intensity in the range where depletion saturation of the illuminated volume occurs.[18] Alternatively, the cross section can be obtained from the detachment signal, whether saturation occurs or not, if the light power, the light spatial distribution, and the ion spatial distribution are known. This is an essential characteristic of the technique for occasions when the product of cross section and light intensity is too small to reach saturation. In the present measurements, both techniques have been used and give mutually consistent results.

II. EXPERIMENTAL PROCEDURE

The Penning ion trap uses a uniform magnetic field and the electric field from three axially symmetric electrodes to confine the ions.[19] The trap used in these experiments has been described previously.[20] For the present measurement, the F^- ions were produced in the trap by means of dissociative attachment of slow electrons to CF_4 gas which was leaked into the vacuum system at a pressure of approximately 2×10^{-8} Torr. After filling the trap with ions, the ion signal was measured by driving the axial motion and observing the currents induced on the ring electrode. The light source was a pulsed 1064-nm Nd:YAG laser operating at a repetition rate of 20 Hz, and the ions were illuminated with light propagating transversely to the axis of the trap for a period of time ranging from 9 to 13 sec. The three-, two-, and one-photon-detachment cross sections were measured using the laser's fundamental frequency and its harmonics. After illumination, the ion signal was measured and the photodetachment ratio was computed.

The power of the light pulses was varied by means of a half-wave plate and a linear polarizer, and the light was monitored after the trap by a volume-absorbing disk calorimeter (Scientech 0101). The YAG laser pulse energy was held fixed throughout the measurements in order to avoid changes of the temporal width, the focus geometry, and the beam position. The temporal profile of the light pulses of each harmonic was measured using a fast photodiode and a 1-GHz-bandwidth oscilloscope. Photographs of the scope display were digitized and fitted to Gaussian distributions. The full width at half maximum were 14.7, 11.5, and 8.3 nsec for the fundamental (ir), second harmonic (green), and third harmonic (uv), respectively. Measurements of the cross sections were made using the laser in both multimode and single-longitudinal-model operation. The single-mode oscillation of the laser was achieved by means of a commercial injection seeding system (Spectra Physics Model 6300). The temporal envelope of the pulse as well as the spatial intensity distribution at the focus did not change significantly when switching the laser from multimode to single-mode oscillation.

The light pulses were focused into the center of the ion trap by one of three spherical lenses which were employed during the course of measurements. The focal lengths of the lenses were 43, 55, and 70 cm, and focus sizes for each experimental arrangement were obtained by measuring the light transmitted through a 6-μm slit which was stepped across the focus. The resulting focus intensity data were fitted to models based on Gaussian or truncated Lorentzian distribution functions. The maximum intensities of the focused beams were 3.2×10^{11} W/cm^2 for the ir, 6.4×10^{10} W/cm^2 for the green, and 1.3×10^{7} W/cm^2 for the uv. The measured confocal parameters, or twice the Rayleigh ranges, of the light beams were always greater than the size of the ion cloud. This is convenient, since in most cases to good approximation the light intensity can be considered constant over the ion cloud in the direction of light propagation.

III. ANALYSIS

While the range of focus of the light was larger than the ion-cloud diameter, the diameter of the focus was substantially smaller, and a single pulse illuminates only a small portion of the ion cloud. Since the period of ion oscillation in the trap is much longer than the duration of a laser pulse, the ions are essentially stationary for the duration of the pulse. The rate equation for the density of the ions in the illuminated region during the light pulse is $d\rho/dt=-\Gamma_k\rho$, where ρ is the ion density and Γ_k is the photodetachment rate. From lowest-order perturbation theory, the transition rate Γ_k for a kth-order, nonresonant process can be defined in terms of generalized cross section and the kth power of photon flux $\Gamma_k=\sigma_k F^k$. The photon flux F is presumed to be a function separable in space and time $F(\mathbf{x},t)=F_0 g(t)D(\mathbf{x})$, where F_0 is the maximum flux, $g(t)$ is the temporal envelope, and $D(\mathbf{x})$ is the spatial distribution. At this point, enhancement factors due to intensity fluctuations are not explicitly included,[21] but these are considered later. The solution of the rate equation for ion density in the illuminated portion of the ion cloud, integrated over the duration of the laser pulse, is

$$\rho(\mathbf{x})=\rho_0(\mathbf{x})\exp[-\sigma_k F_0^k \tau_k D^k(\mathbf{x})] , \tag{1}$$

where $\tau_k=\int g^k(t')dt'$ is the kth-order pulse width, $\rho(\mathbf{x})$ is the ion density after the pulse, and $\rho_0(\mathbf{x})$ is the ion density before the pulse. The number of ions detached by a single light pulse is[17]

$$N_d=\int \rho_0(\mathbf{x})(1-e^{-\sigma_k F_0^k \tau_k D^k(\mathbf{x})})d^3\mathbf{x} . \tag{2}$$

Figure 1 shows the ratio of ions surviving illumination

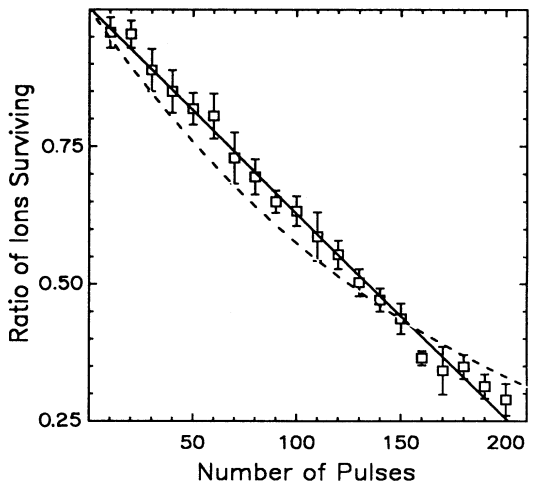

FIG. 1. Ratio of ions surviving illumination as a function of the number of light pulses for two-photon detachment. The solid line and dashed lines show the results of straight line and exponential fits, respectively. When the focus size is small compared to the size of the ion cloud, data for one-, two-, and three-photon detachment all exhibit linear behavior until more than half of the ion cloud is depleted.

with tightly focused green light at fixed power and varying number of pulses. The straight line is the result of a fit to the data for low depletion. The linear behavior for more than 50% depletion of the ions suggests that the ion cloud redistributes itself after each pulse to maintain constant density at the center of the trap. While the range of linearity varies, all the data taken with small focus diameters are consistent with linear behavior for at least 50% depletion of the ions. (Other data show that when the focus size is comparable to the size of the ion cloud, the ion number decays exponentially with increasing number of pulses.) For the purposes of extracting cross sections, a detailed understanding of the linear behavior is not required, but the model used to analyze the data must reflect the linear decay. As long as the focus size is small and the ion depletion is less than 50%, the cloud decays linearly and the number N of ions surviving after m light pulses is, $N=N_0-mN_d$, where N_0 is the initial number of ions. In the approximation that the spatial intensity variation along the direction of light propagation is small over distances corresponding to the size of the ion cloud, and with the assumption that the light pulse has azimuthal symmetry about the direction of propagation, the ratio R of ions surviving after m pulses is

$$R=1-2\pi\eta m\int_0^\infty (1-e^{-\sigma_k F_0^k \tau_k D^k(r)})r\,dr\ , \qquad (3)$$

where $\eta=(1/N_0)\int\rho_0(\mathbf{x})dz$ is the normalized column density. If the trap and ion-production parameters are kept fixed, η, which is independent of the light parameters, should remain constant for all of the data. Thus, the values of η provide a test of the consistency of the data from run to run. Another useful parameter is the effective fraction of ions f illuminated by a single pulse. For kth-order detachment, $f_k=(1/N_0)\int\rho_0(\mathbf{x})D^k(\mathbf{x})d^3\mathbf{x}$. Near saturation, $1/f_k$ is the approximate number of light pulses needed to completely deplete the ion population. If the size of the focus is small and the range of the focus is large compared to the cloud, f_k and η are simply related by $f_k=\eta\int D^k(x,y)dxdy$, i.e., f is equal to η multiplied by the effective area of the focus.

IV. RESULTS

Equation (3) was fitted to data in which the detachment ratio was measured as a function of light-pulse power. When the maximum intensity is low, the exponential term in the integrand of Eq. (3) can be approximated by the first two terms of its Taylor expansion. In this limit, the detachment ratio $1-R$ should be proportional to the kth power of the light intensity. Figure 2 shows photodetachment data for three-photon and two-photon detachment ratios versus light intensity on logarithmic scales. The slope of the fitted line is very close, as expected below saturation, to the order of the detachment process. The slopes obtained from the data shown in Fig. 2 are 2.86(10) and 1.91(6), for three- and two-photon detachment, respectively. Figure 3 shows higher intensity data, where saturation is important, obtained using a shorter-focal-length lens. Saturation due to population depletion by the light pulse is included in Eq. (3).

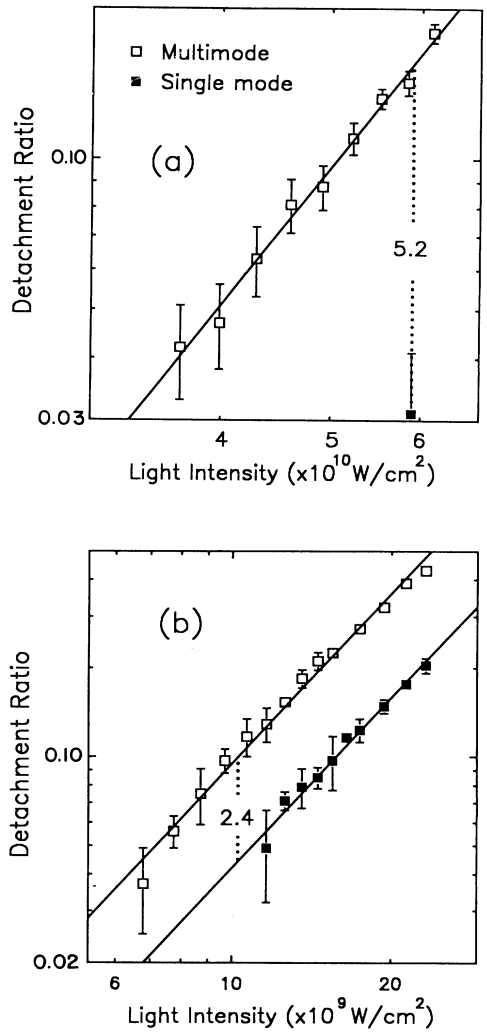

FIG. 2. Log-log plot of the detachment ratio as a function of peak light intensity at relatively low light intensities for (a) three-photon detachment and (b) two-photon detachment. Fitted slopes of (a) 2.86(10) and (b) 1.91(6) show the order of nonlinearity for each process. Enhancement factors for multimode light of (a) 5.2(13) and (b) 2.4(2) are obtained by direct comparison of detachment ratios at fixed light intensity.

Without saturation the data in Fig. 3 would show a much more rapid decrease in ion ratio as the light intensity increases. Data taken with either low- or high-intensity light (or both) can be fitted to Eq. (3), as shown in Fig. 2 and Fig. 3, and these fits give consistent values for the cross sections.

The low- and high-intensity data can be combined by taking into account the light focus size and the number of pulses used. The data for two-photon detachment with multimode light pulses from Figs. 2(b) and 3(b) are combined in Fig. 4 using a simple "top-hat" model for the light intensity distribution. The low-intensity data were taken with 260 light pulses and the high-intensity data with 180 pulses. The low-intensity data from Fig. 2(b) are adjusted, using only the separately measured spot

sizes and number of pulses, to their position relative to the higher-intensity data from Fig. 3(b). The straight line in Fig. 4 is the result of the fit to the low-intensity data taken from Fig. 2(b). The extension of the dynamic range over that available for a single data set and the presence of saturation in the higher-intensity data are obvious.

Almost all of the data for three-photon detachment and some of the data for two-photon detachment were obtained with multimode pulses. Data obtained with both single-mode and multimode pulses are shown in Fig. 2. At lower intensities the three-photon detachment rate for multimode pulses was 5.3(13) times greater than for single-mode pulses, and the two-photon detachment rate for multimode pulses was 2.4(2) times greater than the rate for single-mode pulses. These multimode enhancement factors are in agreement with the factors obtained from the results of high intensity data shown in Fig. 3. The multimode enhancement factor taken from Fig. 3 is $(I_s/I_m)^k$, where I_s is the single-mode light intensity and I_m is the multimode light intensity which photodetach the same fraction of ions. The data in Fig. 3 give the enhancement factors 6.2(5) for three-photon detachment 2.5(2) for two-photon detachment. The average measured enhancement factors for all data are 5.7(6) for three-photon detachment and 2.4(2) for two-photon detachment. If the amplitude distribution of the multimode light is Gaussian, these numbers should be $k!$ for a kth order process,[22] which has been verified in multiphoton ionization of noble gases and alkali-metal vapors.[21,23] The measured enhancement factor for three-photon detachment is consistent with $k!=6$, but the measured two-photon enhancement factor is greater than $k!=2$. Enhancement factors greater than $k!$ can arise from amplitude distributions within the pulses which are broader than Gaussian.

In extracting cross sections from the data, we have treated the two- and three-photon cases differently. For two-photon detachment, where we have good single-mode data, these data provide a value of the cross section, and the multimode data give a value for the enhancement factor. Single-mode operation of the laser was verified by measurements of linewidths and temporal

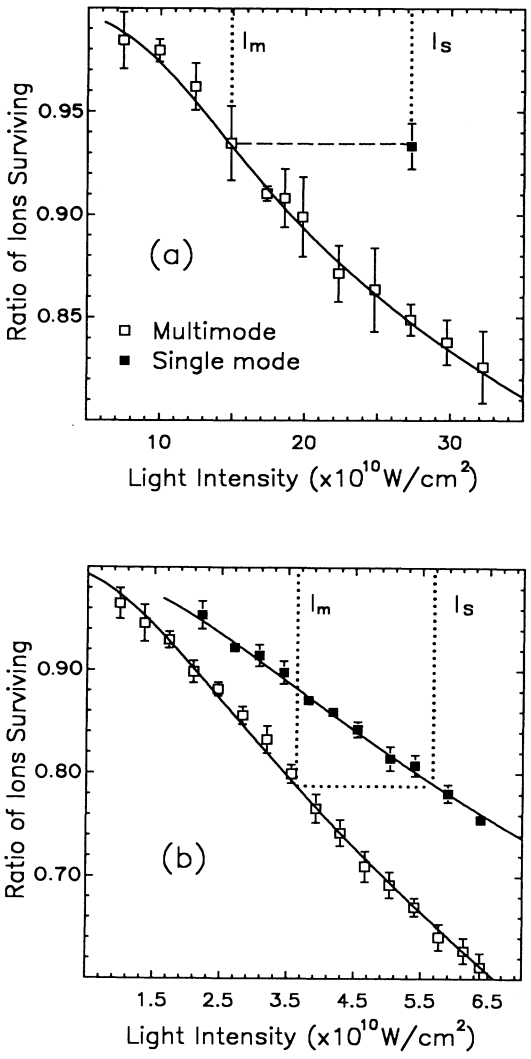

FIG. 3. Ratio of ions surviving detachment as a function of peak light intensity at relatively high intensities obtained with tightly focused light for (a) three-photon detachment and (b) two-photon detachment. For multiphoton detachment, tightly focused light pulses photodetach more ions at lower light powers and the detachment rate begins to saturate as the power increases. Enhancement factors for multimode light of 6.2(5) and 2.5(2) for three- and two-photon detachment, respectively, are obtained from these data using the expression $(I_s/I_m)^k$, where I_s and I_m are the single and multimode intensities, respectively, which detach the same fraction of ions.

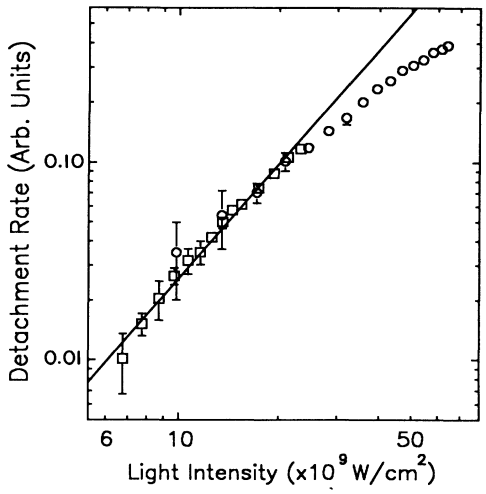

FIG. 4. Log-log plot of the relative detachment ratio for two-photon detachment with multimode light as a function of peak light intensity. The low-intensity data from Fig. 2(b) (open squares) and high-intensity data from Fig. 3(b) (open circles) are combined in this plot by taking into account light focus sizes and the number of light pulses used for detachment. The straight line is the fit to the low-intensity data from Fig. 2(b). Saturation is clearly evident.

TABLE I. Photodetachment cross sections for detached electron energies of 0.097 eV (one and three photon) and 1.26 eV (two photon). The results obtained in this work are compared with theoretical results and, in the case of one-photon detachment, with previous experiments. The results of the frozen-core free-electron (FCFE) and frozen-core Hartree-Fock (FCHF) calculations are taken from Ref. 1, the central-potential model (CPM) results are from Ref. 5, and relativistic random-phase approximation (RRPA) result is from Ref. 29. Values marked by an asterisk were obtained by interpolation between or extrapolation of the points presented in the reference.

Process	This work	Other expts.	FCFE[a]	FCHF[a]	CPM[b]	RRPA[c]	Units
three photon	$7.9^{+6.6}_{-3.6}$		7.1	10*			10^{-83} cm^6 sec^2
two photon	2.0(7)		3.8	1.7*	4.3		10^{-50} cm^4 sec
one photon	2.8(5)	1.8(5)[d] 2.8(7)*[e]			3.6*	2.4	10^{-18} cm^2

[a]Reference 1.
[b]Reference 5.
[c]Reference 29.
[d]Reference 27.
[e]Reference 28.

profile. For three-photon detachment, most of the data on the enhancement factor was obtained under conditions where the spatial distribution of the light was not easily characterized and therefore could not be used to provide a cross section. Multimode data with carefully measured spatial distributions were used together with the measured enhancement factor of 5.7(6) to extract a value for the cross section. The results for the cross sections are presented in Table I.

A principle source of uncertainty in the measured cross sections was the uncertainty of focused light intensity obtained from the measurements of spot size, temporal width, and light-pulse power. The effect of this uncertainty on the measured cross section increases with the order of the detachment. Uncertainties in the cloud distribution enter as uncertainty in the column density η. The uncertainties in the cross sections resulting from the uncertainty in the cloud distribution were relatively small. Two methods of obtaining η were used. The first method was to introduce η as an adjustable parameter in the least-squares fits to data which included the effects of saturation. As discussed above, only the parameters of the light pulse need to be added to data which includes saturation in order to extract a cross section. The other method was to calculate η from measurements of the ion-cloud size. The ion-density distribution was obtained by measuring ion loss rates due to detachment with sharply focused uv pulses which were scanned over the cloud. An example of data obtained from this kind of measurement is shown in Fig. 5. These detachment data were fitted to Gaussian density distributions for the cloud in the directions along and perpendicular to the axis of the trap. At the high temperatures characteristic of ions clouds in our experiments, the Debye length is larger than the extent of the cloud, and a Gaussian function should be a good approximation to the density distribution.[24] The solid line in Fig. 5 is the result of a fit which demonstrates that the data are well represented by a Gaussian function. The η calculated from the ion distribution deviated by approximately 10% from the value obtained by fitting saturated detachment data to Eq. (3).

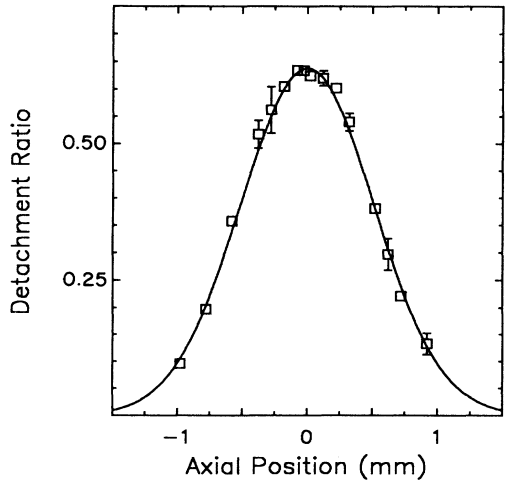

FIG. 5. Detachment ratio as a function of axial position of the light focus for sharply focused ultraviolet-light pulses. The solid line shows the results of a fit to a Gaussian. Such data are used to calculate a normalized column density at the center of the cloud as discussed in the text.

We have estimated the sizes of the error resulting from the assumption that the ion cloud is small compared to the range of the light focused. For most of the data the error is negligible. However, due to experimental constraints, the confocal parameter was larger than the cloud by only a factor of 2 for the three-photon data. For these data, a correction to account for the noncylindrical light beam was calculated for each data point and both the corrected data and the uncorrected data were fitted to Eq. (3) to obtain a cross section. The cross sections from the corrected data were used as the final results and the approximately 15% differences between the cross sections from the corrected and uncorrected data were added to the estimated error. Another possible source of systemat-

ic error discovered in the earlier experiments on Cl^- is ion repopulation due to dissociative attachment of photodetached electrons to the gas used in ion production.[8] This effect was significant for the Cl^- experiment, but is not in the present case since the attachment rate for thermal electrons to CF_4 is nine orders of magnitude smaller than the rate for attachment to CCl_4.[25] The structure in the cross section due to the presence of a magnetic field[26] should not have a large effect on the results. The detached electron energy for one- and three-photon detachment, where we are closest to threshold, is approximately 0.1 eV or 800 times the electron cyclotron energy. Estimating the possible size of the magnetic-field-induced modulations in the cross section suggests that any effects should be less than 5%. The dependence of the photodetachment rate on the orientation of the light polarization with respect to the magnetic field was measured and no dependence was observed. The data presented here were taken with light linearly polarized perpendicular to the magnetic field.

Table I presents theoretical and the other experimental results for F^- photodetachment cross sections in addition to the present results. The measured three-photon cross section is in agreement with both the fixed-core free-electron (FCFE) and the fixed-core Hartree-Fock (FCHF) results of Crance.[1] On the other hand, the measured two-photon cross section is near the FCHF result, but clearly less than the FCFE result and the central-potential model (CPM) result of Robinson and Geltman.[5] Calculations by Jiang and Starace[3] for Cl^- and by L'Huillier and Wendin[4] for I^- also produce results that lie below the FCFE results for the respective ions. Taken together, our experimental result and the other theoretical results suggests that the FCFE calculation give a two-photon cross section that is too high, and that the FCHF cross section is more accurate. The measured one-photon cross section is larger than the cross section measured by Mandl,[27] but in agreement with and somewhat more precise than the recent measurement of Vacquie, Gleizes, and Sabsabi.[28] The relativistic random-phase approximation (RRPA) calculation of Radojevic, Kelly, and Johnson,[29] extrapolated to low energy, is in agreement with the experimental result.

V. CONCLUSION

These experiments have demonstrated the applicability of the stored-ion technique to measurements of absolute cross sections for single- and multiphoton detachment. At the present level of precision, the multiphoton measurements do not reflect the limitations of the stored-ion technique, but rather more directly reflect the present uncertainties in the measurements of the light intensities. The single-photon cross section is limited by the knowledge of the ion distribution in the trap, but the ion-trap technique can be extended beyond this level of precision. The measurements have produced cross sections for multiphoton detachment from F^-, and the measured two-photon cross section in particular provides a critical point of comparison for different theoretical calculations.

ACKNOWLEDGMENTS

This work was supported in part by the National Science Foundation.

[1]M. Crance, J. Phys. B **20**, 6553 (1987).
[2]M. Crance, J. Phys. B **20**, L411 (1987).
[3]T. F. Jiang and A. F. Starace, Phys. Rev. A **38**, 2347 (1988).
[4]A. L'Huillier and G. Wendin, J. Phys. B **21**, L247 (1988).
[5]E. J. Robinson and S. Geltman, Phys. Rev. **153**, 4 (1967).
[6]J. L. Hall, E. J. Robinson, and L. M. Branscomb, Phys. Rev. Lett. **14**, 1013 (1965).
[7]C. Blondel, R.-J. Champeau, A. Crubellier, C. Delsart, H. T. Duong, and D. Marinescu, Europhys. Lett. **4**, 1267 (1987).
[8]R. Trainham, G. D. Fletcher, and D. J. Larson, J. Phys. B **20**, L777 (1987).
[9]For example, K. C. Smyth and J. I. Brauman, J. Chem. Phys. **56**, 5993 (1972); R. C. Stoneman and D. J. Larson, Phys. Rev. A **35**, 2928 (1987); D. J. Larson, C. J. Edge, R. E. Elmquist, N. B. Mansour, and R. Trainham, Phys. Scr. **T22**, 183 (1988).
[10]P. S. Drzaic and J. I. Brauman, Chem. Phys. Lett. **83**, 508 (1981); F. K. Meyer, J. M. Jasinski, R. N. Rosenfeld, and J. I. Brauman, J. Am. Chem. Soc. **104**, 663 (1982).
[11]E. N. Ensberg and K. B. Jefferts, Astrophys. J. **195**, L89 (1975).
[12]J. Eyler, J. Am. Chem. Soc. **98**, 6831 (1976).
[13]F. L. Walls and G. H. Dunn, J. Geophys. Res. **79**, 1911 (1974); R. D. DuBois, J. B. Jeffries, and G. H. Dunn, Phys. Rev. A **17**, 1314 (1978).
[14]M. H. Prior, R. Marrus, and C. R. Vane, Phys. Rev. A **28**, 141 (1983); D. A. Church, Phys. Scr. **T22**, 164 (1988).
[15]M. D. McGuire and E. N. Fortson, Phys. Rev. Lett. **33**, 737 (1974).
[16]S. E. Barlow, G. H. Dunn, and M. Schauer, Phys. Rev. Lett. **52**, 902 (1984).
[17]T. A. Lehman and M. M. Bursey, *Ion Cyclotron Resonance Spectrometery* (Wiley, New York, 1976).
[18]J. Morellec, D. Normand, and G. Petite, At. Mol. Phys. **18**, 97 (1982).
[19]H. G. Dehmelt, Adv. At. Mol. Phys. **3**, 53 (1967); **5**, 109 (1969); D. J. Wineland, W. M. Itano, and R. S. Van Dyck, Jr., *ibid.* **19**, 135 (1983).
[20]D. J. Larson and R. Stoneman, Phys. Rev. A **31**, 2210 (1985).
[21]C. Lecomte, G. Mainfray, C. Manus, and F. Sanchez, Phys. Rev. A **11**, 1009 (1975).
[22]P. Lambropoulous, Adv. At. Mol. Phys. **12**, 87 (1976).
[23]L. A. Lompre, G. Mainfray, C. Manus, and J. P. Marinier, J. Phys. B **14**, 4307 (1981).
[24]D. J. Wineland, J. J. Bollinger, Wayne M. Itano, and J. D. Prestage, J. Opt. Soc. Am. B **2**, 1721 (1985).
[25]L. G. Christophorou, D. L. McCorkl, and A. A. Christodoulides, *Electron-Molecule Interactions and Their Applications*, edited by L. G. Christophorou (Academic, New York, 1984), Vol. 1.
[26]W. A. M. Blumberg, W. M. Itano, and D. J. Larson, Phys.

Rev. A **19**, 139 (1979); D. J. Larson and R. Stoneman, *ibid.* **31**, 2210 (1985); C. H. Greene, *ibid.* **36**, 4236 (1987); O. H. Crawford, *Production and Neutralization of Negative Ion Beams (Brookhaven, 1986)*, Proceedings of the Fourth International Symposium on the Production and Neutralization of Negative Ion Beams, AIP Conference Proceedings No. 158, edited by J. G. Alessi (AIP, New York, 1987), p. 663.

[27]A. Mandl, Phys. Rev. A **3**, 251 (1971).

[28]S. Vacquie, A. Gleizes, and M. Sabsabi, Phys. Rev. A **35**, 1615 (1987).

[29]V. Radojevic, H. P. Kelly, and W. R. Johnson, Phys. Rev. A **35**, 2117 (1987); V. Radojevic (private communication).